

Analytical design of an Offner imaging spectrometer

X. Prieto-Blanco, C. Montero-Orille, B. Couce, and R. de la Fuente

*Departamento de Física Aplicada
Escola Universitaria de Óptica e Optometría
Universidade de Santiago de Compostela
15782 Galicia, Spain
jaloraul@usc.es*

Abstract: We present the analytical design of an imaging spectrometer based on the three-concentric-mirror (Offner) configuration. The approach presented allows for the rapid design of this class of system. Likewise, high-optical-quality spectrometers are obtained without the use of aberration-corrected gratings, even for high speeds. Our approach is based on the calculation of both the meridional and the sagittal images of an off-axis object point. Thus, the meridional and sagittal curves are obtained in the whole spectral range. Making these curves tangent to each other for a given wavelength results in a significant decrease in astigmatism, which is the dominant residual aberration. RMS spot radii less than $5\ \mu\text{m}$ are obtained for speeds as high as $f/2.5$ and a wavelength range of $0.4\text{-}1.0\ \mu\text{m}$. A design example is presented using a free interactive optical design tool.

© 2006 Optical Society of America

OCIS codes: (050.1950) Diffraction gratings, (120.6200) Spectrometers and spectroscopic instrumentation, (220.1000) Aberration compensation, (220.4830) Optical systems design.

References and links

1. N. Gat, "Imaging Spectroscopy using tunable filters: a review," Proc. SPIE **4056**, 50-64 (2000). G. A. Shaw, H. K. Burke, "Spectral imaging for remote sensing", Lincoln Laboratory Journal **14**, 3-28, (2003).
2. P. Mouroulis and M. McKerns, "Pushbroom imaging spectrometer with high spectroscopic data fidelity: experimental demonstration," Opt. Eng. **39**, 808-816 (2000).
3. D. Kwo, G. Lawrence, and M. Chrisp, "Design of a grating spectrometer from a 1:1 Offner mirror system," Proc. SPIE **818**, 275-279 (1987).
4. M.P. Chrisp, *Convex diffraction grating imaging spectrometer*, U.S. Patent 5,880,834.
5. W.J. Smith, *Modern Optical Engineering* (McGraw-Hill, Inc., New York, 1990).
6. H. Beutler, "The theory of the concave grating," J. Opt. Soc. Am. **35**, 311-350 (1945). W. T. Welford, "Aberration theory of gratings and grating mountings" in *Progress in Optics*, E. Wolf, ed., Vol. IV, 241-280, North-Holland, Amsterdam (1965).
7. M.C. Hutley, *Diffraction Gratings* (Academic Press, London, 1982).
8. G.A. Korn and T.M. Korn, *Mathematical Handbook for Scientists and Engineers*, second edition (Dover Publications, Inc., Mineola, New York, 2000), Chap. 17.1.
9. A copy of the macro used in this paper can be obtained by contacting the authors.
10. J.M. Howard, "Optical Design using computer graphics," Appl. Opt. **40**, 3225-3231 (2001).
11. OSLO is a registered trademark of Lambda Research Corporation, 80 Taylor Street, P.O. Box 1400, Littleton, Mass. 01460.
12. C. Davis, J. Bowles, R. Leathers, D. Korwan, TV Downes, W. Snyder, W. Rhea, W. Chen, J. Fisher, P. Bissett, and R.A. Reisse, "Ocean PHILLS Hyperspectral Imager: Design, Characterization, and Calibration," Opt. Express **10**, 210-221 (2002).

1. Introduction

Hyperspectral imaging spectrometers are radiation sensors that provide a collection of spectral images of an inhomogeneous scene. This allows the spectral signature for each object point to be determined. They can be applied to perform many different tasks such as accurate mapping of wide areas, object identification and recognition, target detection, process monitoring and control, clinical diagnosis imaging and environment assessment and management. Application areas include forestry, geology, agriculture, medicine, security, manufacturing, colorimetry, oceanography, ecology and others[1].

In this paper we are concerned with a particular hyperspectral imager: the Offner-like spectrometer. This spectrometer offers some advantages over other spectrometers used in pushbroom imaging spectrometry: low chromatic aberrations, a compact size with low optical distortion, and a high speed[2]. Right now several Offner-like hyperspectral instruments are available. However, an analytical procedure for designing Offner imagers is not presented in the literature. Usually the designs are done by numerical optimization using some kind of optical design software[2][3]. Only recently Chrisp et al.[4] have suggested one design strategy, however their solution is not general and only astigmatism for a given wavelength is canceled. The aim of this work is to provide a more general solution which allows to reduce low order aberrations over the whole wavelength range of the spectrometer. Our approach allows the analytical design of a well-corrected Offner spectrometer with a large entrance aperture. Furthermore the suggested procedure can be implemented in a free lens design software doing the design process very easy.

The standard Offner spectrometer is made of three spherical concentric elements (two concave mirrors and one convex grating). Some solutions have been proposed to optimize the optical quality of such a system. They include tilting or decentering of some elements, and the usage of either toroidal reflective optics or aberration corrected gratings. In general these solutions lead to more expensive and harder to build spectrometers. Our design proposal is applied to the standard Offner spectrometer. So we can obtain simpler, easier to align and cheaper spectrometers. It is a further advantage in addition to the above mentioned ones.

The study of an optical system with an axis of symmetry (the optical axis) is usually performed by means of an analytical expansion of the wavefront around this axis[5]. The result obtained up to second order corresponds to the paraxial approximation. The first correction corresponds to the so-called Seidel aberrations. The study of higher order aberrations allows further refinements. Obviously this task turns to be more involved each time we study a new aberration order. In an Offner spectrometer the entrance slit must be well separate from the center of curvature of the grating to avoid vignetting (see Fig. 1). The analytical design of such a system using the standard approach is a formidable task. Fortunately we can save a lot of effort if we perform the wavefront expansion around another preferred direction. It may be the central ray of the cone of light emerging from an off-axis point. This type of analysis has been carried out to study aberrations in concave gratings[6]. It can be applied immediately to convex gratings and to spherical mirrors as a special case, and therefore to the standard Offner spectrometer. Section 2 presents the fundamentals of the design proposal. Vignetting is not considered because of its complexity. Vignetting is analyzed in Section 3. Finally in Section 4 a specific design procedure is showed as well as a practical example.

2. Theory of the design

The spectrometer discussed in this paper is shown in Fig. 1. It consists of two concave mirrors and one convex grating. The coordinate system is centered at the curvature center of the grating and the z-axis crosses its geometrical center. The object is a slit parallel to y-axis. This slit is imaged by the three elements onto several images each one corresponding to a different

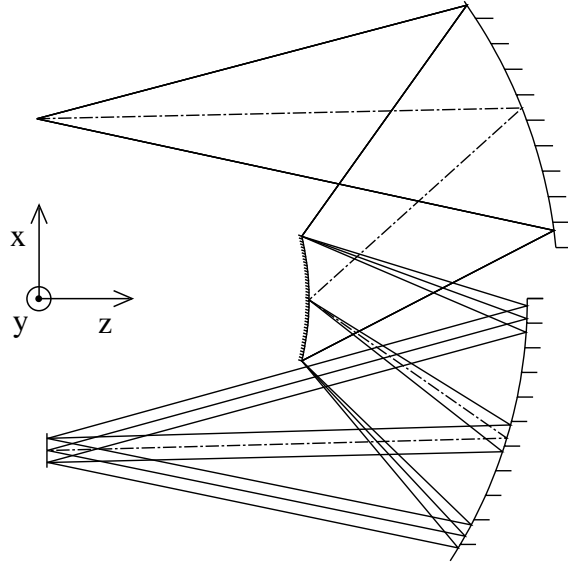


Fig. 1. Offner configuration for an imaging spectrometer. The object is at the top left. It is a slit parallel to y-axis. The grating lies upon the convex mirror and its grooves are also parallel to y-axis. The reference ray is plotted in dot-dashed line.

wavelength. The grating grooves are parallel to y-axis. The grating is the aperture stop and is not aberration corrected. That is, groove size is a constant when projected over a chord parallel to x-axis. To study the imaging properties of this system we will first focus our attention on the most general element: the grating. Next we will extend our analysis to the full system. The directions of diffracted light of the grating satisfy the Bragg relation:

$$\sin \theta + \sin \theta' = m \lambda p, \quad (1)$$

where θ is the incidence angle, θ' the diffraction angle for the maximum of order m , λ the wavelength and p the number of grooves by unit of length. The usual sign convention has been used (see for example [5]). The meridional image of an off-axis object point produced by a reflective grating satisfies[7]

$$\frac{\cos^2 \theta}{r} + \frac{\cos^2 \theta'}{r'_M} = \frac{\cos \theta + \cos \theta'}{R} \quad (2)$$

and the sagittal image verifies

$$\frac{1}{r} + \frac{1}{r'_S} = \frac{\cos \theta + \cos \theta'}{R}. \quad (3)$$

In these Eqs. R is the curvature radius of the grating; r and $r'_{M,S}$ are the distances from the incidence point of the reference ray on the grating to the object and to both the meridional (r'_M) and the sagittal (r'_S) image point (see Fig. (2)). A particular design corresponds to the Rowland's condition[6][7]:

$$r = R \cos \theta \quad \Rightarrow \quad r'_M = R \cos \theta'. \quad (4)$$

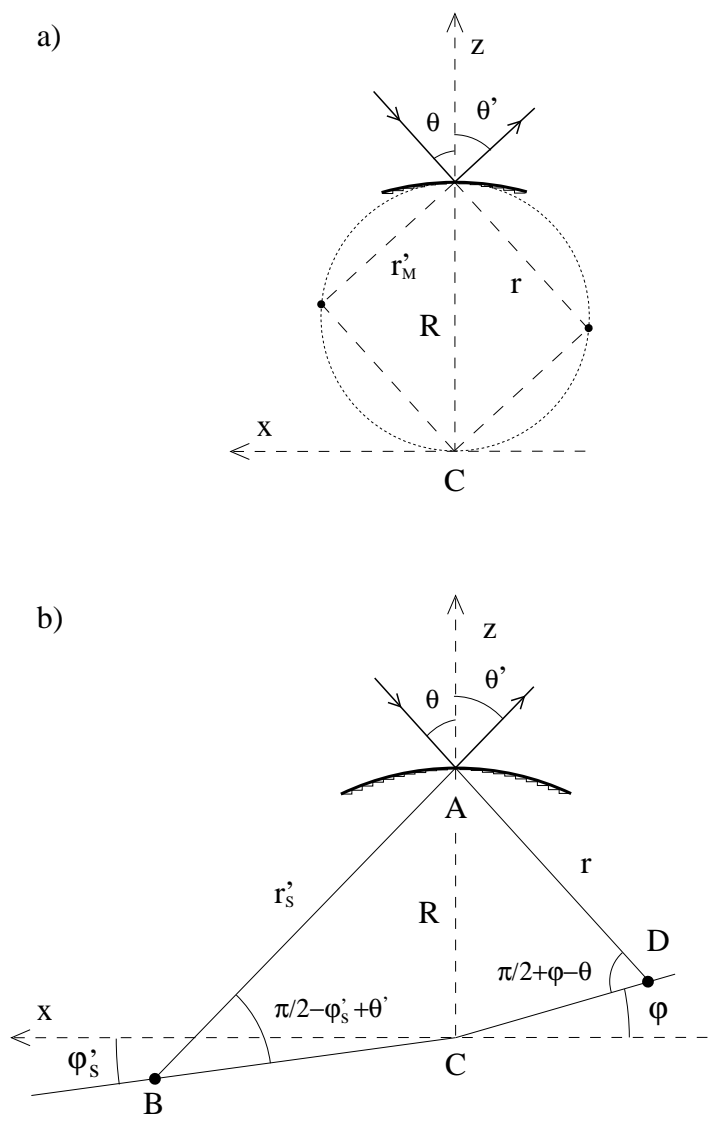


Fig. 2. a) Virtual object and meridional image location on the Rowland circle. b) Schematic to calculate sagittal image location through the grating for a virtual object point.

In this case both object and meridional image lie on the circle of radius $R/2$ that contains the center of curvature of the grating and the incidence point (Rowland circle) as Fig. 2(a) shows. We stress that all the above Eqs. also holds for mirrors ($m=0$). It is advisable that Rowland's condition is satisfied because it ensures a meridional image free of coma[6]. However it is clear from Eq. (3) that the sagittal image does not lie in general on this circle. That makes the astigmatism the most important aberration. However as we will show, by a suitable combination of the three elements of the Offner spectrometer, both images can be matched not only for one specific wavelength but also for near ones.

First let us deduce an expression that holds for the sagittal image produced by every element. It will be useful for further calculations. In Fig. 2(b) we have drawn the grating and both the object (D) and the image (B) locations. From the triangles ACB and ACD, using the sine theorem we get

$$\frac{1}{r} = \frac{\cos(\varphi - \theta)}{R \cos \varphi}$$

$$\frac{1}{r'_S} = \frac{\cos(\varphi'_S - \theta')}{R \cos \varphi'_S}. \quad (5)$$

The substitution of Eqs. (5) in Eq. (3) leads to the following invariant (K) for the sagittal image:

$$K = \sin \theta \tan \varphi = -\sin \theta' \tan \varphi'_S. \quad (6)$$

Note that for a mirror $\varphi = \varphi'_S$, that is, object, curvature center, and image locations are aligned. It is also true for a grating ($m \neq 0$) if object point is on the x-axis.

Now let us consider the three elements together. As the Rowland condition implies a coma free image, a sufficient condition to have a good final meridional image is that object point (the slit center) and both final and intermediate images lie on the Rowland circle of each element. This is the case for both mirrors and grating being concentric provided that the object point is located on the first Rowland circle. We stress that this ensures that the image for each wavelength lies on its own Rowland circle no matter the dispersive properties of gratings. Therefore hereinafter we will assume a concentric configuration. Let us put this condition in a mathematical form. Consider Fig. 3 where we have drawn the Rowland circle of the three elements, the common curvature center (C), the object point (O), and both intermediate and final (I_M) meridional images laying on such circles. The object lies on the first Rowland circle if the angle between CO and the reference ray is $\pi/2$. That follows from the geometric property which holds that a triangle is rectangle if its hypotenuse is the diameter of its circumscribed circle. Taking the quadrangle AOCD we get

$$\frac{\pi}{2} - 2\theta_1 + (\pi - \theta_2) + \frac{\pi}{2} + \varphi = 2\pi \quad \Rightarrow \quad \varphi = \theta_2 + 2\theta_1. \quad (7)$$

Note that according to the sign convention $\theta_1 < 0$. Furthermore the distance CO verifies

$$CO = R_1 \sin \theta_1 = -R_2 \sin \theta_2, \quad (8)$$

where the last equality holds because of the intersection of first and second Rowland circles at the meridional image of the primary mirror. Eq. (7) -or Eq. (8)- is the necessary and sufficient condition, expressed in polar coordinates, for the object point lies on the Rowland circle of the first mirror. In the same way we obtain the following mathematical conditions for the location of the final meridional image:

$$\frac{\pi}{2} - 2\theta_3 + (\pi + \theta'_2) + \frac{\pi}{2} - \varphi'_M = 2\pi \quad \Rightarrow \quad \varphi'_M = \theta'_2 - 2\theta_3 \quad (9)$$

$$CI_M = R_2 \sin \theta'_2 = R_3 \sin \theta_3. \quad (10)$$

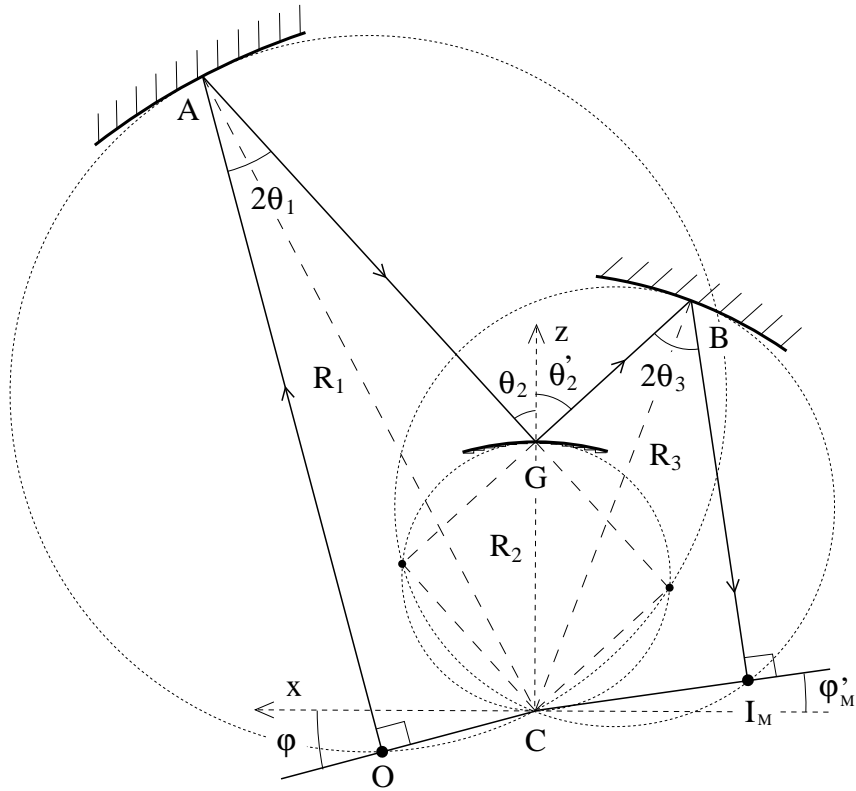


Fig. 3. Rowland circles for the concentric Offner spectrometer showing meridional image locations. Center of curvature of the three elements (C) and both object (O) and image (I_M) locations are indicated.

With regard to sagittal image locations we show them in Fig. 4. As we have discussed above object polar angle equals sagittal image polar angle in both mirrors. So we can relate polar angles of both object point and final sagittal image with incidence and reflection angles on the grating through Eq. (6):

$$\sin \theta_2 \tan \varphi = -\sin \theta'_2 \tan \varphi'_S. \quad (11)$$

On the other hand (see Fig. 4) radial locations of sagittal images can be related to meridional ones by

$$CI_S = \frac{CI_M}{\cos(\varphi'_M - \varphi'_S)} \quad (12)$$

Note that this equation holds for every wavelength because the meridional image for each wavelength lies on its own Rowland circle. As soon as we have located the final meridional and sagittal images it is straightforward to determine the astigmatism as the distance between them (see Fig. 4):

$$\text{Astig} = CI_S \sin(\varphi'_M - \varphi'_S). \quad (13)$$

So the condition to achieve a null astigmatism for a given wavelength -which could be the central one ($\bar{\lambda}$) in the spectral range of the spectrometer- is

$$\bar{\varphi}' = \bar{\varphi}'_S = \bar{\varphi}'_M = \bar{\theta}'_2 - 2\bar{\theta}_3. \quad (14)$$

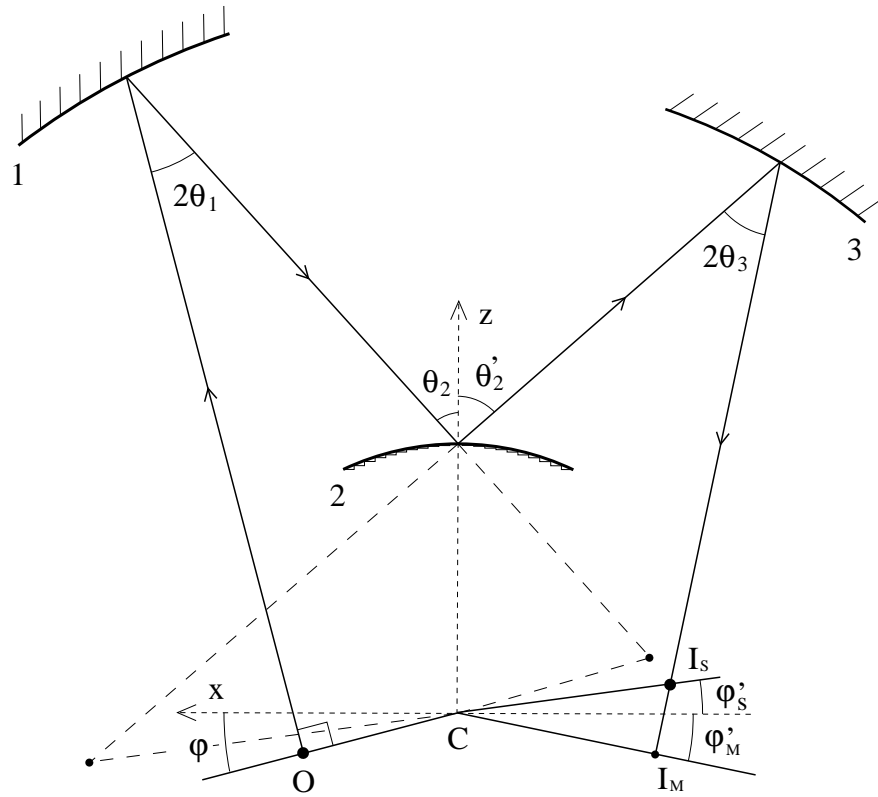


Fig. 4. Location of the sagittal images throughout the concentric Offner spectrometer. For comparison the location of the final meridional image is also shown.

If this is the case it is obvious from Eq. (12) that

$$\overline{CI} = \overline{CI}_M = \overline{CI}_S. \quad (15)$$

A particular solution is obtained if $\bar{\varphi} = \bar{\varphi}' = \theta_2 + 2\theta_1 = \bar{\theta}'_2 - 2\bar{\theta}_3 = 0$, that is, the reference ray in both the object and image space and the z-axis are parallel. Such a particular solution leads to the design proposed by Chrisp et al. [4].

The meridional and sagittal images are in fact curves rather than points because of grating dispersion (see Fig. 5). Equation (14) only assures null astigmatism for wavelength $\bar{\lambda}$, where the curves intersect. However there is still one degree of freedom that can be used to improve the design. For example, we can cancel astigmatism for another wavelength. We have explored this possibility but it leads to Eqs. that do not make the design easy. Another possibility is to make the meridional and the sagittal curves tangent to each other at wavelength $\bar{\lambda}$. As we show in section 4, this condition assures a high matching of these curves in the whole spectral range of the spectrometer. Mathematically, the tangency condition implies that the astigmatism (the distance between curves along reference rays) is at least second order in wavelength. Thus, we impose

$$\left. \frac{dAstig}{d\lambda} \right|_{\bar{\lambda}} = 0 \Rightarrow \left. \frac{d(\varphi'_M - \varphi'_S)}{d\theta'_2} \right|_{\bar{\theta}'_2} = 0, \quad (16)$$

where we use Eq. (13) and (14). The derivative of the meridional angle is determined by means

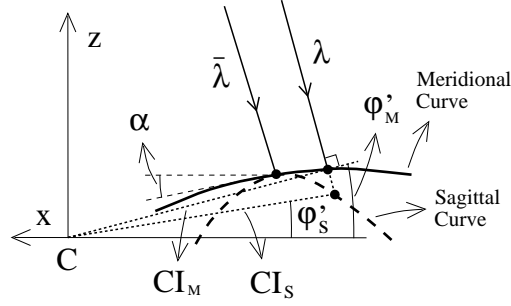


Fig. 5. Location of both meridional and sagittal final images for a wavelength λ another than the central one ($\bar{\lambda}$). The meridional image lies on its own Rowland's circle. Both meridional and sagittal curves are drawn.

of Eq. (9) and (10):

$$\frac{d\varphi'_M}{d\theta'_2} = 1 - 2 \frac{\tan \theta_3}{\tan \theta'_2} \quad (17)$$

whereas Eq. (11) allows to obtain

$$\frac{d\varphi'_S}{d\theta'_2} = - \frac{\sin \varphi'_S \cos \varphi'_S}{\tan \theta'_2}. \quad (18)$$

Combining the last two Eqs. and using Eq. (14) to eliminate θ'_2 we write Eq. (16) as

$$\tan(\bar{\varphi}' + 2\bar{\theta}_3) - 2 \tan \bar{\theta}_3 + \frac{\sin 2\bar{\varphi}'}{2} = 0. \quad (19)$$

This equation can not be solved in the present form. By using simple trigonometric identities the first and the third terms can be written as functions of $\tan \bar{\varphi}'$. After some algebra we obtain a cubic equation in $\tan \bar{\varphi}'$:

$$\frac{\sin^3 \bar{\theta}_3}{\cos \bar{\theta}_3} + \tan \bar{\varphi}' - \tan \bar{\theta}_3 \cos(2\bar{\theta}_3) \tan^2 \bar{\varphi}' + \frac{1 + 2 \sin^2 \bar{\theta}_3}{2} \tan^3 \bar{\varphi}' = 0. \quad (20)$$

This equation only has a real solution for $\tan \bar{\varphi}'$. Moreover for typical values of $\bar{\theta}_3$ ($|\bar{\theta}_3| < 25^\circ$) $\bar{\varphi}'$ is less than 0.1 rad so that it can be solved quickly by an iterative method. The solution at n-order is given by

$$\tan \bar{\varphi}'_n = - \frac{\sin^3 \bar{\theta}_3}{\cos \bar{\theta}_3} + \tan \bar{\theta}_3 \cos(2\bar{\theta}_3) \tan^2 \bar{\varphi}'_{n-1} - \frac{1 + 2 \sin^2 \bar{\theta}_3}{2} \tan^3 \bar{\varphi}'_{n-1}, \quad (21)$$

with $\bar{\varphi}'_0 = 0$.

The image produced by the Offner spectrometer at wavelength $\bar{\lambda}$ is determined by $\bar{\varphi}'$ and CI . However we also have to determine the tilt angle of the image plane. We choose the image plane to be tangent to the meridional curve at $\bar{\lambda}$ (hence, also tangent to the sagittal curve). So the tilt angle with respect to the x-axis correspond to angle α in Fig. 5. To obtain α we first find β , the angle between the tangent to the image curves and the position vector \vec{CI}_M at $\bar{\lambda}$. As CI_M and φ' are the polar coordinates of the meridional curve we have (see for example [8])

$$\tan \beta = CI_M \frac{d\varphi'_M}{dCI_M} \Big|_{CI} = \bar{CI} \frac{\frac{d\varphi'_M}{d\theta'_2} \Big|_{\bar{\theta}'_2}}{\frac{dCI_M}{d\theta'_2} \Big|_{\bar{\theta}'_2}} = \tan \bar{\theta}'_2 - 2 \tan \bar{\theta}_3, \quad (22)$$

where Eq. (10) and Eq. (17) are used. Now, taking into account the sign convention we have $\alpha = \beta + \varphi'$. Thus combining Eq. (14), (19) and (22) we obtain

$$\alpha = \bar{\varphi}' - \arctan\left(\frac{\sin 2\bar{\varphi}'}{2}\right). \quad (23)$$

To complete the analytical study of the Offner spectrometer we derive a final relationship which connect the size of the spectrometer to the grating density. For that we write Eq. (1) for wavelengths at the boundaries of the spectral range (λ^- , λ^+) and subtract them:

$$(\sin \theta_2'^+ - \sin \theta_2'^-) = mp(\lambda^+ - \lambda^-) = mp\Delta\lambda. \quad (24)$$

Doing the same thing for Eq. (10) we have

$$R_2(\sin \theta_2'^+ - \sin \theta_2'^-) = CI_M^+ - CI_M^- \simeq h_{spec}, \quad (25)$$

where h_{spec} is the size of the spectral image and the last approximation can be made because of the small values which φ' takes. The combination of these last Eqs. provides

$$R_2 = \frac{h_{spec}}{mp\Delta\lambda} \quad (26)$$

which relates in a proportional way the grating density to the size of the spectrometer (R_2 can be regarded as a scaling factor).

For a given $\bar{\theta}_3$ and after choosing the desired specifications of the spectrometer (spectral range, image size, f-number and size of the device) the above Eqs. allow to obtain its geometric parameters. Namely, both curvature and aperture radius of elements, grating density, both slit and image locations, and image plane tilting. On the other hand the value of θ_3 is fixed through the vignetting analysis. This is considered in the following section.

3. Vignetting analysis

In an Offner spectrometer vignetting of the incident cone of rays can take place at three locations. We show them in Fig. 6 for $|R_1| > |R_3|$. As soon as the specifications of the spectrometer have been stated whether or not vignetting occurs depends on the decentering of the line object from the curvature center of the mirrors. According to our analysis such a decentering (see Fig. 3) is related to the angle of incidence θ_1 . As θ_1 is related to $\bar{\theta}_3$ let us choose the last one as the free parameter whose value determines whether or not rays are stopped by some mirror.

The vignetting analysis involves the calculation of trajectories of several rays and its intersection around the three locations mentioned above (see Fig. 6). This analysis must be done for the wavelength which is going to suffer more vignetting. That wavelength corresponds to the light which diffracts more toward the object. The conditions for no vignetting can be written in a general form as:

$$(x_i^2 + z_i^2)^{1/2} > -R_2 \quad i = 1, 2 \quad (27)$$

$$(x_3^2 + z_3^2)^{1/2} < \min(-R_1, -R_3). \quad (28)$$

However the calculation of x_i and z_i as a function of $\bar{\theta}_3$ is long and tedious. Moreover the Eqs. derived do not allow to calculate $\bar{\theta}_3$ in an explicit way. As our aim is to provide an easy to use design procedure, we follow a more practical strategy. We program an interactive graphical tool[9] by using the macro language of a lens design software. The tool is written following the work of Howard[10] but applying the Eqs. presented in Section 2. Howard proposes some interactive routines to design optical systems by visual checking of their performance. In our case the interactivity facilitates the search for the smaller incident angle $\bar{\theta}_3$ which leads to no vignetting. This also allows for rapid design. Some results using such a software are shown in the following Section.

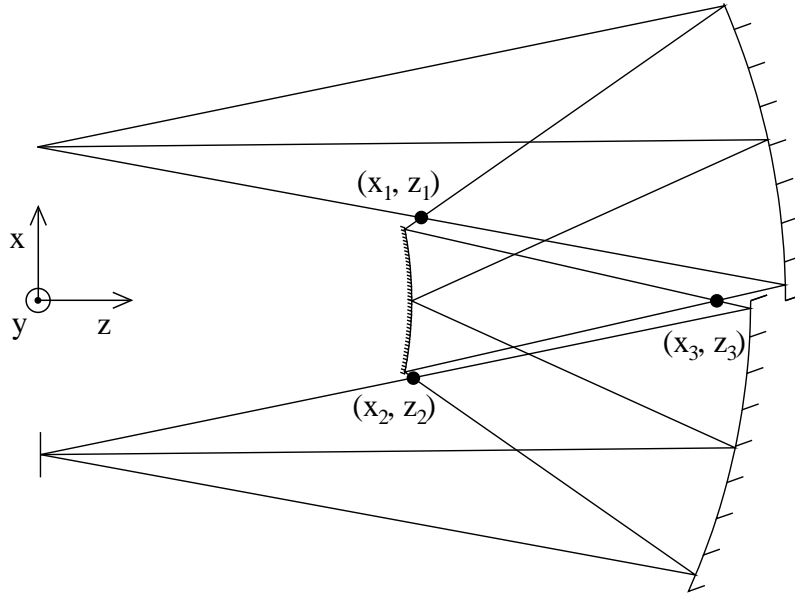


Fig. 6. Locations (1, 2, and 3) where vignetting may appear for small $\bar{\theta}_3$ angles

4. Design procedure

The general design procedure is sketched in Fig. 7. The procedure starts assuming an initial -close to zero- angle $\bar{\theta}_3$. Then the Eqs. derived above are used in the indicated order. As soon as all the parameters are determined calculation of vignetting is carried out. If vignetting exists then $|\bar{\theta}_3|$ must be increased, the procedure starts again, and so on. The procedure ends when $|\bar{\theta}_3|$ is high enough to avoid vignetting. As we have mentioned in the previous section calculation of

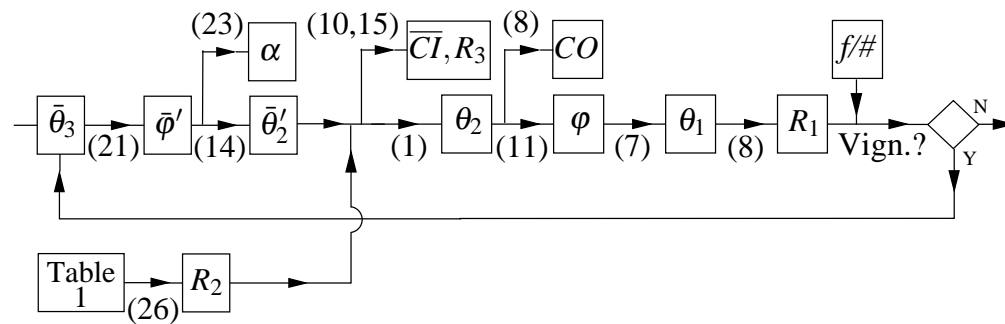


Fig. 7. Steps for carrying out the spectrometer design according to the theory presented in Section 2. The equation number used at each step is indicated.

vignetting is not direct. So we have implemented the design procedure in the macro language of OSLO-EDU, a free version of OSLO lens design software[11]. OSLO provides a macro language (CCL) for building interactive interfaces as well as the conventional tools for lens design.

As an example let us design the spectrometer whose specifications are in Table 1. We have chosen the spectral range and both the spectral and spatial sizes according to the typical specifications of 2/3" CCD sensors. The groove density corresponds to a standard value and allows a compact spectrometer. Finally we have chosen a f/2.6 speed because it is similar to those of comparable imaging spectrometers[2][12]. The design wavelength is picked out to be the central one but it is not a must. In cases where the optical quality for λ^+ and λ^- is very different from each other another design wavelength should be selected.

Table 1. Specifications of the spectrometer to be designed.

Spectral range ($\lambda^- - \lambda^+$)	400-1000 nm
Design wavelength ($\bar{\lambda}$)	700 nm
Spectral image size (h_{spec})	6.6 mm
Spatial image size (h)	8.8 mm
f-number	2.6
Diffraction order (m)	-1
Grating density (p)	150 l/mm

We show in Fig. 8 the most significant outputs of OSLO for this design. The *Slider Window* is the interactive window to input the specifications. Particularly angle $\bar{\theta}_3$ can be modified until no vignetting occurs. In this case it does for $|\bar{\theta}_3| > 13.437^\circ$ but to allow for building tolerances it is safer to let $|\bar{\theta}_3| = 15^\circ$. Whether or not vignetting occurs is checked in the

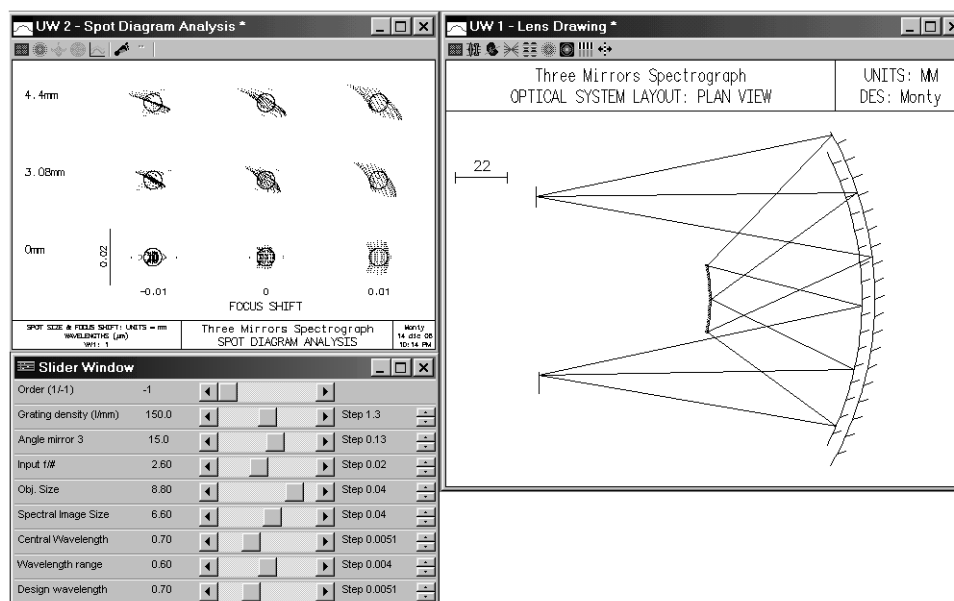


Fig. 8. Outputs of the implementation in OSLO-EDU of the design procedure. We show the results for the spectrometer whose specifications are in Table 1.

Lens Drawing window. The rays corresponding to the light which is diffracted more towards the object are plotted in this window ($\lambda^+ = 1 \mu\text{m}$ in our example). Finally the *Spot Diagram*

Analysis window shows the image spots for this wavelength and for three field points (0 mm, 3.08 mm and 4.4 mm). The Airy's disk boundary is also plotted as a black circle. The optical quality of the design is obvious regarding this figure. A complete analysis reveals that the worst RMS spot radius for both wavelengths considered (0.4 μm , 0.7 μm , and 1.0 μm) and for the three field points mentioned is 4.74 μm which is close to the diffraction limit (3.18 μm for $\lambda^+ = 1 \mu\text{m}$). A spectral resolution less than 0.9 nm can be achieved with such a spot size and for the given spectral range. Moreover if we decrease $|\bar{\theta}_3|$ to 13.5° (which is in the range to avoid vignetting) the worst RMS spot radius is reduced to 3.68 μm and the spectral resolution to less than 0.7 nm. We stress that in both cases we have slightly z-shifted the image plane to get more rounded spots. This shift changes the spot radii very little, actually it increases slightly the worst RMS value. The design prescription for $|\bar{\theta}_3| = 15^\circ$ is given in Table 2. We

Table 2. Prescription data

R_1	-142.66 mm	φ	0.842°
R_2	-73.33 mm	$\bar{\varphi}'$	1.024°
R_3	-137.26 mm	α	$\sim 0^\circ$
CO	43.23 mm		
CI	35.53 mm		

have also evaluated two typical distortions present in pushbroom spectral imagers: smile (image curvature for monochromatic light) and keystone (change of magnification with wavelength). They are as low as expected for this class of spectrometer[2]. Smile is $\sim 0.1 \mu\text{m}$ and keystone $\sim 0.3 \mu\text{m}$ which correspond to 0.833% and 2.5%, respectively, for a pixel size of 12 μm .

To show the quality of this approach we plot in Fig. 9 the worst RMS spot radius versus f-number for the specifications in Table 1. For each f-number $|\bar{\theta}_3|$ is the smaller angle that leads to no vignetting. It can be seen from this figure that reasonable results are obtained even for very fast speeds. For example a worst RMS spot radius of $\sim 12 \mu\text{m}$ is obtained for $f/2.0$ and $m=1$. This spot radius is similar to the RMS value of the commercially available VS-15 spectrometer which uses an aberration corrected grating[12]. Even though the spots for high apertures may look not so good this design procedure is still useful. It provides a starting point for both numerical optimization by removing the concentric constrain and specific grating design. This potential improvements have not been checked because it is beyond the scope of the present paper.

5. Conclusions

We show that using a simple analytical approach it is easy to design high aperture imaging spectrometers based on the Offner relay. Our approach allows for every wavelength to reduce the astigmatism in a great amount. Thus high optical quality spectrometers are obtained - even diffraction-limited- without use of specific aberration corrected gratings nor numerical optimization through expensive optical software. Furthermore we propose a design procedure according to the theoretical results. It is used to design a particular spectrometer. Both to easily take into account vignetting and make faster the design itself we implement this procedure using a free version of OSLO lens design software. It results in a powerful tool for designing Offner imaging spectrometers of excellent quality in a short time.

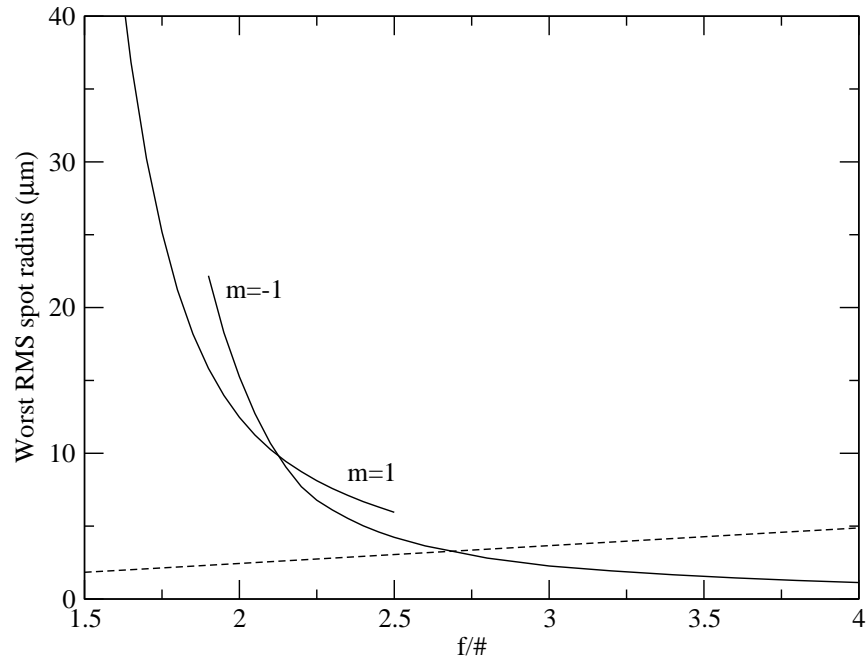


Fig. 9. Worst RMS spot radius versus f-number for $m=\pm 1$ diffraction orders (solid lines) and the specifications from Table 1. The diffraction limit (dashed line) is also represented for wavelength $\lambda^+=1000$ nm. Note that diffraction limits the minimum spot size for $f/\# > 2.7$.

Acknowledgments

This work has been carried out in the framework of the contracts VEM2003-20088-C04-03 and PGIDIT04PXIC22201PN.